Наносистеми, наноматеріали, нанотехнології
Nanosistemi, Nanomateriali, Nanotehnologii
2025, т. 23, № 1, сс. 27–36
https://doi.org/10.15407/nnn.23.01.0027

PACS numbers: 36.40.Cg, 36.40.Vz, 71.15.Mb, 71.15.Nc, 73.21.La, 81.05.Zx, 81.07.Ta

Ab initio Calculations of Electronic Properties of Non-Stoichiometric Cd_mTe_n Clusters

I. V. Semkiv[1], L. R. Deva[1], P. A. Shchepanskyi[2], M. Ya. Rudysh[3], N. Y. Kashuba[1], N. T. Pokladok[1], and A. I. Kashuba[1]

[1]*Lviv Polytechnic National University,*
12, Bandera Str.,
UA-79013 Lviv, Ukraine
[2]*Ivan Franko National University of Lviv,*
19, Dragomanov Str.,
UA-79000 Lviv, Ukraine
[3]*Jan Długosz University in Częstochowa,*
13/15, Armii Krajowej Al.,
42-200 Częstochowa, Poland

Non-stoichiometric Cd_mTe_n ($m \neq n$: $Cd_{13}Te_4$, Cd_4Te_{13}, $Cd_{19}Te_{16}$, $Cd_{16}Te_{19}$, $Cd_{38}Te_{28}$, and $Cd_{28}Te_{38}$) clusters with spherical form and diameter of 1, 1.4, and 1.6 nm are studied. These Cd_mTe_n clusters have T_d point-group symmetry. All calculations including geometry optimization and energy spectra of the Cd_mTe_n clusters are made using density functional theory (DFT). The GGA + PBE approximation is used to describe the exchange–correlation energy of the electron subsystem with Hubbard corrections (GGA + U). Structural properties, bond length, symmetry and electronic properties like the HOMO–LUMO gap, binding energy, and electronegativity are analysed.

Подано результати досліджень нестехіометричних кластерів Cd_mTe_n ($m \neq n$: $Cd_{13}Te_4$, Cd_4Te_{13}, $Cd_{19}Te_{16}$, $Cd_{16}Te_{19}$, $Cd_{38}Te_{28}$ і $Cd_{28}Te_{38}$) зі сферичною формою та діяметром у 1, 1,4 й 1,6 нм. Досліджувані кластери Cd_mTe_n описано точковою групою симетрії T_d. Усі розрахунки, включаючи оптимізацію геометрії й енергетичні спектри кластерів Cd_mTe_n, виконано з використанням теорії функціоналу густини. Для опису обмінно-кореляційної енергії використано наближення GGA + PBE з Габбардовими поправками (GGA + U). Проаналізовано структурні властивості, довжину зв'язку, симетрію й електронні властивості, такі як енергетична щілина HOMO–LUMO, енергія зв'язку й електронеґативність.

Key words: non-stoichiometric clusters, CdTe, semiconductor, HOMO–LUMO gap, binding energy, electronegativity.

Ключові слова: нестехіометричні кластери, CdTe, напівпровідник, енергетична щілина HOMO–LUMO, енергія зв'язку, електронеґативність.

(Received 12 February, 2024)

1. INTRODUCTION

Nanocrystalline semiconducting materials of II–VI group offer unique electronic and optical properties attributed to the so-called quantum confinement effects [1]. The optical properties of such compounds can be adjusted by altering the dimensions of the nanoparticles. CdTe clusters (also in the form of the quantum dots (QDs)), are important II–VI group semiconducting materials with a narrow bulk band gap ($\cong 1.44$ eV) [1] and a high excitation Bohr radius (7.3 nm) [2, 3]. QDs based on CdTe have potential applications in novel light emitters, next-generation solar cells, sensing, and biomedical diagnostics [4].

In the present work, the gap between highest occupied molecular orbital (HOMO) and lowest unoccupied molecular orbital (LUMO), binding energy and electronegativity of the non-stoichiometric Cd_mTe_n ($m \neq n$) clusters have been calculated. The information about studies of physical properties of the CdTe clusters was found in the literature [2, 4–18]. In these works also are reports on the density functional theory (DFT) calculations of electronic and optical properties of Cd_mTe_n ($m \neq n$ [13, 18], $m = n$ [10, 13, 16, 17, 18]) clusters. Particularly, the LDA [18], GGA + PBE [10, 13, 18], and B3LYP [10, 16] functionals were used for DFT calculations. The Cd_4Te_{13}, $Cd_{13}Te_{14}$, $Cd_{14}Te_{13}$, $Cd_{19}Te_{29}$, $Cd_{19}Te_{28}$, and $Cd_{79}Te_{80}$ clusters were studied in [13]. In Ref. [18], the $Cd_{13}Te_{16}$, $Cd_{16}Te_{13}$, $Cd_{16}Te_{19}$, and $Cd_{19}Te_{16}$ non-stoichiometric clusters were used for studies of the electronic properties.

The paper is organized as follows. The next section introduces the calculation techniques used. The first subsection in the third section reports the main results of the electronic band energy structure of bulk CdTe. Structural properties of non-stoichiometric Cd_mTe_n ($m \neq n$: $Cd_{13}Te_4$, Cd_4Te_{13}, $Cd_{19}Te_{16}$, $Cd_{16}Te_{19}$, $Cd_{38}Te_{28}$, and $Cd_{28}Te_{38}$) clusters are elucidated in the second subsection of the third section. The third subsection in the third section is the study of the HOMO–LUMO gap, binding energy, and electronegativity of non-stoichiometric Cd_mTe_n clusters. Finally, the conclusions are drawn in the last section.

2. METHODS OF CALCULATION

All calculations including geometry optimization and energy spectra

were made using DFT, which was implemented in Quantum Espresso package [19]. Density functional GGA + PBE was used to describe the exchange–correlation energy of the electronic subsystem with Hubbard corrections (GGA + U). Unfortunately, for strongly correlated materials, including CdTe, the standard DFT with GGA (PBE) functional will underestimate the band gap. The easiest way to get the results closer to experimental ones is to use a so-called 'scissor' operator, which leads to the band gap changing by shifting the conduction band into the region of higher energies [20] or to use Hubbard U correction [21].

Firstly, structure optimization and calculation of electron band energy structure were made for bulk CdTe. This calculation was performed to estimate the value of Hubbard corrections. The value $E_{\text{cut-off}} = 660$ eV for the energy of cutting-off the plane waves was used in our calculations. The electronic configurations of $5s^2 4d^{10}$ for Cd and $5s^2 5p^4$ for Te atoms formed the valence electron states. The self-consistent convergence of the total energy was taken as $5.0 \cdot 10^{-6}$ eV/atom. Geometry optimization of the lattice parameters and atomic coordinates was performed using the Broyden–Fletcher–Goldfarb–Shanno (BFGS) minimization technique with the maximum ionic Hellmann–Feynman forces within 0.01 eV/Å, the maximum ionic displacement within $5.0 \cdot 10^{-4}$ Å, and the maximum stress within 0.02 GPa.

Based on the optimized structure of the bulk CdTe, the Cd_mTe_n clusters (in spherical form) with diameter (D) of 1, 1.4, and 1.6 nm were built. The convergence criteria for energy and force were set to $\cong 3 \cdot 10^{-4}$ eV and $\cong 5 \cdot 10^{-2}$ eV/Å respectively for all the calculations. To describe accurately the electronic spectrum, two Hubbard corrections were selected for the studied objects: for d-orbitals of Cd ($U_{4d} = 5.80$ eV) and p-orbitals of Te ($U_{5p} = 2.55$ eV).

3. RESULTS AND DISCUSSIONS

3.1. Electron Band Energy Structure of Bulk CdTe

In Figure 1, the full energy band diagrams of the CdTe crystal are shown along the highly symmetric lines of the 1-st Brillouin zone (BZ: W(0.500, 0.250, 0.750), L(0.500, 0.500, 0.500), Γ(0, 0, 0), X(0.500, 0, 0.500), and K(0.375, 0.375, 0.750)). The energy position of the Fermi level (E_F) is aligned with 0 eV. Analysis of the results of theoretical calculations of the energy band spectrum shows that the smallest band gap is localized in the centre of the BZ (the Γ point) for GGA and GGA + U calculations. This means that the crystal is characterized by a direct energy band gap. The estimated band gap for the GGA calculation is 0.494 eV. It is less than

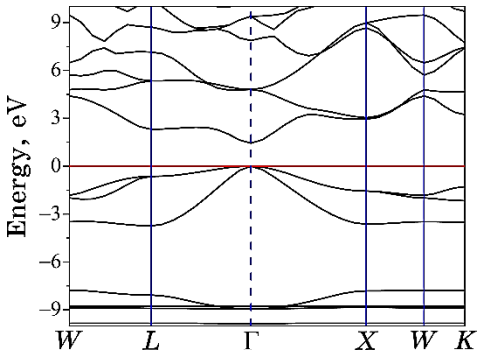

Fig. 1. Electron band energy structure of bulk CdTe (calculated using GGA + U).

the appropriate value obtained experimentally (≅ 1.44 eV [1]). Using the Hubbard correction $U_{4d} = 5.80$ eV for Cd and $U_{5p} = 2.55$ eV for Te atoms, we obtained the band gap of 1.438 eV for the bulk CdTe, perfectly consistent with the experimental data [1].

3.2. Structural Properties of Non-Stoichiometric Cd_mTe_n Clusters

Based on the optimized structure of the bulk CdTe, the Cd_mTe_n spherical clusters with different diameters between 1 and 1.6 nm were built (see Fig. 2). The clusters were further optimized using the parameters reported in the second section. The non-stoichiometric Cd_mTe_n clusters before and after optimizations are shown in the Fig. 2 (detailed information is in the figure). These Cd_mTe_n clusters have T_d point group symmetry. The average Cd–Te bonds lengths (l) in the clusters are listed in Table 1. As seen in Table 1, Cd_mTe_n clusters with rich content of Cd ($m/n > 1$) have larger average Cd–Te bonds lengths than the Te-content rich clusters ($m/n < 1$).

3.3. HOMO–LUMO Gap, Binding Energy, and Electronegativity of Non-Stoichiometric Cd_mTe_n Clusters

To study the solvent effects on the energy position of the HOMO, LUMO, and HOMO–LUMO gap, we performed the geometry optimization of the clusters in the presence of the solvents. A comparison of the calculated value of the HOMO, LUMO, and HOMO–LUMO gap for non-stoichiometric $Cd_{13}Te_4$ and Cd_4Te_{13} clusters shows the gaps to be very similar for water, acetone, and ethanol. Based on these results, only water was used as a solvent in calculations for

other clusters.

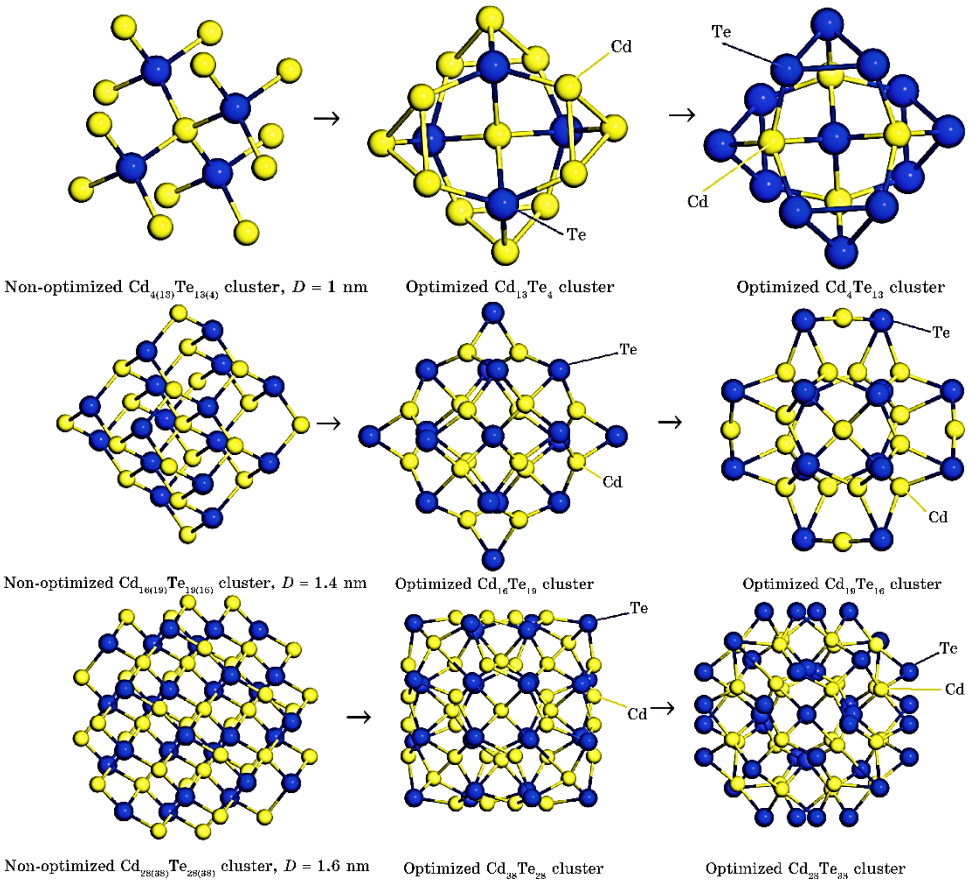

Fig. 2. Structure of non-stoichiometric Cd_mTe_n clusters before (non-optimized) and after optimizations.

TABLE 1. Average Cd–Te bond length for studied clusters (PGS states for point group symmetry).

Cd_mTe_n cluster	m/n	PGS	l, Å
$Cd_{13}Te_4$	13/4	T_d	2.99750
Cd_4Te_{13}	4/13	T_d	2.89275
$Cd_{16}Te_{19}$	16/19	T_d	2.86100
$Cd_{19}Te_{16}$	19/16	T_d	2.87800
$Cd_{28}Te_{38}$	28/38	T_d	2.85840
$Cd_{38}Te_{28}$	38/28	T_d	2.88257

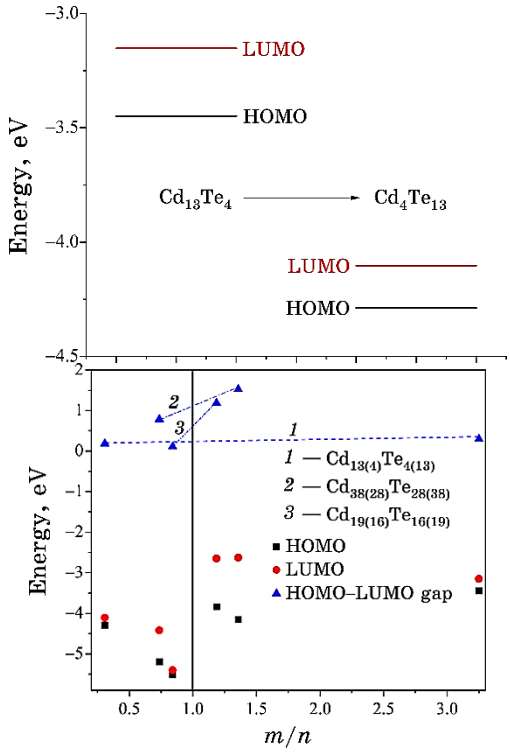

Fig. 3. Left panel—energy position of the HOMO, LUMO and HOMO–LUMO gap for $Cd_{13}Te_4$ and Cd_4Te_{13} clusters (solvent—water). Right panel—energy position of the HOMO, LUMO and HOMO–LUMO gap for non-stoichiometric Cd_mTe_n clusters (details in figure).

The energy positions of HOMO and LUMO for $Cd_{13}Te_4$ and Cd_4Te_{13} clusters are shown in Fig. 3 (left panel). In Figure 3 (left panel), one can see that the energy position of HOMO and LUMO decreases while moving from Cd-rich ($Cd_{13}Te_4$) to the Te-rich (Cd_4Te_{13}) clusters. In addition, a higher value of the HOMO–LUMO gap is observed for the Cd-rich cluster ($Cd_{13}Te_4$).

In Table 2, the energy position of the HOMO, LUMO, and HOMO–LUMO gap of non-stoichiometric Cd_mTe_n clusters are listed. For analysis of these results, we used a composition ratio (m/n). In Figure 3 (right panel), the dependence of the energy position of HOMO, LUMO, and HOMO–LUMO gap from the composition ratio is shown. As one can see in Figure 3 (right panel), the HOMO–LUMO gap increases for all cases when the composition ratio changes (transition from Cd-rich to Te-rich cluster). In addition, when the composition ratio m/n is heading to 1 (case of the stoichiometric Cd_nTe_n clusters) this gap increases and goes to a value above

TABLE 2. Electronic properties of non-stoichiometric CdTe clusters in different solvents.

Cd_mTe_n cluster	Solvent	HOMO, eV	LUMO, eV	HOMO–LUMO gap, eV
$Cd_{13}Te_4$	Water	–3.449	–3.152	0.297
$Cd_{13}Te_4$	Ethanol	–3.444	–3.145	0.299
$Cd_{13}Te_4$	Acetone	–3.443	–3.145	0.298
Cd_4Te_{13}	Water	–4.288	–4.103	0.185
Cd_4Te_{13}	Ethanol	–4.290	–4.105	0.185
Cd_4Te_{13}	Acetone	–4.290	–4.105	0.185

TABLE 3. Electronic properties of non-stoichiometric CdTe clusters (solvent—water).

Cd_mTe_n cluster	HOMO, eV	LUMO, eV	HOMO–LUMO gap, eV	E_b, eV	χ, eV
$Cd_{13}Te_4$	–3.444	–3.145	0.299	1.03298	3.2945
Cd_4Te_{13}	–4.288	–4.103	0.185	1.77638	4.1955
$Cd_{16}Te_{19}$	–5.507	–5.398	0.109	2.05143	5.4525
$Cd_{19}Te_{16}$	–3.833	–2.646	1.187	1.92718	3.2395
$Cd_{28}Te_{38}$	–5.201	–4.413	0.788	2.16213	4.8070
$Cd_{38}Te_{28}$	–4.151	–2.625	1.526	1.93342	3.3880

1.526 eV (E_g for $Cd_{38}Te_{28}$). This value (of 1.526 eV) is larger than for bulk CdTe (1.438 eV). The increasing tendency of the energy gap is connected with the quantum-size effect ($D < 2$ nm). In addition, we established that the value for the HOMO–LUMO gap is much higher for clusters with $n > m$.

To estimate the stability of studied clusters, the binding energy was calculated. Binding energy was obtained using Eq. (1) and is listed in Table 3; Table 3 also lists electronegativities, which were calculated based on Eq. (2) [22]:

$$E_b = \left[mE_{total}(\mathrm{Cd}) + nE_{total}(\mathrm{Te}) + E_{total}(\mathrm{Cd}_m\mathrm{Te}_n)\right] / \left[m + n\right]; \quad (1)$$

$$\chi = -\left[\mathrm{HOMO} + \mathrm{LUMO}\right] / 2\,. \quad (2)$$

A comparison of the binding energies of the Cd_mTe_n clusters ($E_b(m/n < 1) > E_b(m/n > 1)$) indicates that the samples with $m/n < 1$ (Te-rich clusters) are more stable than samples with $m/n > 1$ (Cd-rich clusters). In the clusters group with $n > m$, Te atoms are on the surface (see Fig. 2) and hence these structures are energetically favoured [18].

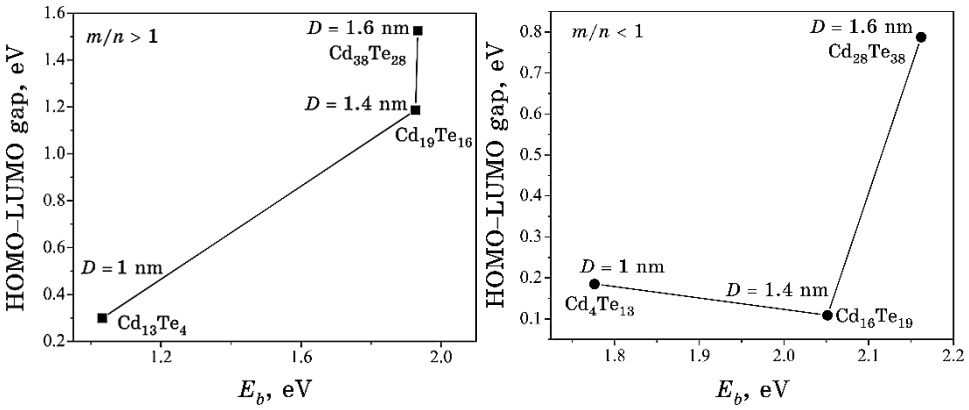

Fig. 4. The relation between HOMO–LUMO gap and E_b for non-stoichiometric Cd_mTe_n clusters (details on figure).

The latter can be related to Jahn–Teller distortion in the $m > n$ clusters. A similar tendency has been observed in non-stoichiometric HgTe [23] and CdTe [18] clusters. However, in our case, the structure symmetry (see Table 1) of the non-stoichiometric Cd_mTe_n clusters was saved (in Ref. [18], [23] symmetry is destroyed after optimization).

The relationship between E_b and HOMO–LUMO gap is presented in Fig. 4. In the case of $m/n > 1$ (see Fig. 4 (left panel)), the increase of E_b is appears along with the increase in the HOMO–LUMO gap, which means that the larger E_b value will have a cluster with a larger band gap. However, in the case of $m/n < 1$ (Te-rich clusters), this dependence (see Fig. 4 (right)) is more difficult. This can be related to the decreasing in the average Cd–Te bond lengths (see Table 1) when the composition ratio changes from $m/n > 1$ on $m/n < 1$.

4. CONCLUSION

First-principle theoretical studies of the electron properties for the non-stoichiometric Cd_mTe_n ($m \neq n$) clusters have been carried out using the reliable techniques of density functional theory and known approximations. Based on these calculations, the energy position of HOMO, LUMO, HOMO–LUMO gap, binding energy, and electronegativity are obtained for the studied clusters.

Structure analysis shows that the Cd_mTe_n clusters with rich content of Cd ($m/n > 1$) have larger Cd–Te average bonds lengths than the Te-content rich clusters ($m/n < 1$). For all clusters, the structure symmetry was saved.

Analysis of the energy properties shows that the solvent (water, acetone or ethanol) does not have effects the energy position of the HOMO, LUMO, and HOMO–LUMO gap. Increasing of the HOMO–LUMO gap when the composition ratio m/n is heading to 1 is observed. Additionally, it was revealed, based on the calculated value of the binding energy, that the samples with $m/n < 1$ (Te-rich clusters) are more stable than samples with $m/n > 1$ (Cd-rich clusters).

This work was supported by the Project for Young Scientists No. 0124U000760 granted by the Ministry of Education and Science of Ukraine.

REFERENCES

1. R. Petrus, H. Ilchuk, A. Kashuba, I. Semkiv, and E. Zmiiovska, *Funct. Mater.*, **27**, No. 2: 342 (2020); https://doi.org/10.15407/fm27.02.342
2. M. Akbari, M. Rahimi-Nasrabadi, S. Pourmasud, M. Eghbali-Arani, H. Reza Banafshe, F. Ahmadi, M. Reza Ganjali, and A. Sobhani nasab, *Ceramics International*, **46**, No. 8: 9979 (2020); https://doi.org/10.1016/j.ceramint.2020.01.051
3. Y.-J. Yang, X. Tao, Q. Hou, and J.-F. Chen, *Acta Biomaterialia*, **5**, No. 9: 3488 (2009); https://doi.org/10.1016/j.actbio.2009.05.002
4. V. Dzhagan, O. Kapush, O. Isaeva, S. Budzulyak, O. Magda, P. Kogutyuk, L. Trishchuk, V. Yefanov, M. Valakh, and V. Yukhymchuk, *Physics and Chemistry of Solid State*, **23**, No. 4: 720 (2022); https://doi.org/10.15330/pcss.23.4.720-727
5. L.-W. Wang and J. Li, *Physical Review B*, **69**, No. 15: 153302(4) (2004); https://doi.org/10.1103/PhysRevB.69.153302
6. A. P. Nicholson, A. H. Munshi, U. Pozzoni, and W. S. Sampath, *2018 IEEE 7th World Conference on Photovoltaic Energy Conversion* (2018), p. 1932–1936; doi:10.1109/PVSC.2018.8547599
7. Y. Mastai and G. Hodes, *J. Phys. Chem. B*, **101**, No. 14: 2685 (1997); https://doi.org/10.1021/jp963069v
8. Y. Masumoto and K. Sonobe, *Physical Review B*, **56**, No. 15: 9734 (1997); https://doi.org/10.1103/PhysRevB.56.9734
9. E. Gharibshahi, *Solid State Communications*, **320**: 114009 (2020); https://doi.org/10.1016/j.ssc.2020.114009
10. B. Rajbanshi and P. Sarkar, *J. Phys. Chem. C*, **120**, No. 32: 17878 (2016); https://doi.org/10.1021/acs.jpcc.6b04662
11. Y. Al-Douri, H. Baaziz, Z. Charifi, R. Khenata, U. Hashim, and M. Al-Jassim, *Renewable Energy*, **45**: 232 (2012); https://doi.org/10.1016/j.renene.2012.02.020
12. J. Li and L.-W. Wang, *Physical Review B*, **72**, No. 12: 125325(15) (2005); https://doi.org/10.1103/PhysRevB.72.125325
13. S. Kr. Bhattacharya and A. Kshirsagar, *Eur. Phys. J. D*, **48**: 355 (2008); https://doi.org/10.1140/epjd/e2008-00114-3
14. S. Baskoutas and A. F. Terzis, *J. Appl. Phys.*, **99**, No. 1: 013708(4) (2006); https://doi.org/10.1063/1.2158502

15. S. K. Haram, A. Kshirsagar, Y. D. Gujarathi, P. P. Ingole, O. A. Nene, G. B. Markad, and S. P. Nanavati, *J. Phys. Chem. C*, **115**, No. 14: 6243 (2011); https://doi.org/10.1021/jp111463f
16. A. E. Kuznetsov and D. N. Beratan, *J. Phys. Chem. C*, **118**, No. 13: 7094 (2014); https://doi.org/10.1021/jp4007747
17. S. C. Boehme, J. M. Azpiroz, Y. V. Aulin, F. C. Grozema, D. Vanmaekelbergh, L. D. A. Siebbeles, I. Infante, and A. J. Houtepen, *Nano Lett.*, **15**, No. 5: 3056 (2015); https://doi.org/10.1021/acs.nanolett.5b00050
18. S. Kr. Bhattacharya and A. Kshirsagar, *Physical Review B*, **75**, No. 3: 035402(10) (2007); https://doi.org/10.1103/PhysRevB.75.035402
19. P. Giannozzi, O. Andreussi, T. Brumme, O. Bunau, M. Buongiorno Nardelli, M. Calandra, R. Car, C. Cavazzoni, D. Ceresoli, and M. Cococcioni, *J. Phys.: Condens. Matter*, **29**, No. 46: 465901 (2017); doi:10.1088/1361-648X/aa8f79
20. A. I. Kashuba, I. V. Semkiv, H. A. Ilchuk, R. Y. Petrus, V. M. Kordan, and S. V. Shyshkovskyi, *J. Optoelectron. Adv. Materials*, **24**, Nos. 9–10: 477 (2022); https://joam.inoe.ro/articles/first-principle-calculations-of-electron-phonon-optic-and-thermodynamic-properties-of-cdse-and-cds-crystals/
21. M. Kovalenko, O. Bovgyra, V. Dzikovskyi, and R. Bovhyra, *SN Applied Sciences*, **2**: 790 (2020); https://doi.org/10.1007/s42452-020-2591-9
22. C.-G. Zhan, J. A. Nichols, and D. A. Dixon, *J. Phys. Chem. A*, **107**, No. 20: 418 (2003); https://doi.org/10.1021/jp0225774
23. X. Q. Wang, S. J. Clark, and R. A. Abram, *Physical Review B*, **70**, No. 23: 235328 (2004); https://doi.org/10.1103/PhysRevB.70.235328